Relative preservation of peripheral lung function in smoking-related pulmonary emphysema: assessment with ^{99m}Tc-MAA perfusion and dynamic ^{133}Xe SPET

Kazuyoshi Suga, Norihiko Kume, Naofumi Matsunaga, Nobuhiko Ogasawara, Kazumi Motoyama, Akiko Hara, Tsuneo Matsumoto

Department of Radiology, Yamaguchi University School of Medicine, Ube, Yamaguchi, Japan

Received 8 January and in revised form 13 March 2000

Abstract. In this study the cross-sectional functional differences between the central and peripheral lung in smokers with pulmonary emphysema were evaluated by lung perfusion and dynamic xenon-133 single-photon emission tomography (SPET). The subjects were 81 patients with a long-term smoking history and relatively advanced emphysema, 17 non-smoker patients with non-obstructive lung diseases and six healthy non-smokers. Regional lung functional difference between the peripheral and central lung was assessed in the upper, middle and lower lung zones by technetium-99m macroaggregated albumin SPET and dynamic ^{133}Xe SPET. The distribution of emphysematous changes was assessed by density-mask computed tomography (CT) images which depicted abnormally low attenuation areas (LAAs) of less than –960 Hounsfield units. Two hundred and eighty-eight (59.2%) lung zones of 63 (77.7%) patients with pulmonary emphysema showed relative preservation of lung function in the peripheral lung, with a curvilinear band of normal perfusion (a stripe sign) and a significantly faster ^{133}Xe half-clearance time ($T_{1/2}$) than in central lung (P<0.0001). Of these lung zones, 256 (88.8%) showed central-dominant LAA distributions on density-mask CT images, but the remaining 32 zones did not show any regional preference in LAA distribution. Conversely, 117 (24.0%) lung zones of 19 (23.4%) patients showed periphery-dominant perfusion defects and LAA distributions, with significantly prolonged $T_{1/2}$ in the peripheral lung area (P<0.0001). The remaining 81 lung zones of the patients with pulmonary emphysema and all the lung zones of the healthy subjects and patients with non-obstructive lung diseases did not show a stripe sign, and no differences were observed in $T_{1/2}$ values and LAA distributions between the central and peripheral lung. Relative preservation of peripheral lung function seems to be a characteristic feature in smoking-related pulmonary emphysema, and may indicate a lower susceptibility of peripheral parenchyma to the development of this disease.

Key words: Lung – Single-photon emission tomography – Technetium-99m macroaggregated albumin – Xenon-133 gas – Pulmonary emphysema

Eur J Nucl Med (2000) 27:800–806

Introduction

Structural differences between peripheral and central lung may result in cross-sectional morphological and functional differences in the development of lung diseases [1, 2]. Clarification of the cross-sectional morphological and functional differences is fundamental to a systemic understanding of the histopathological development of lung diseases. Cigarette smoking is thought to play an important part in the development of pulmonary emphysema, and this disease has been morphologically categorized as central-dominant or periphery-dominant emphysema in microscopic and computed tomography (CT) studies [3, 4, 5, 6]. A high incidence of a "strip" sign on perfusion scintigrams in this disease, which derives from interposed radioactivity between a central perfusion defect and the pleural surface of the lung, may suggest the presence of functional differences between the peripheral and central lung [7, 8, 9, 10, 11, 12, 13]. However, to date cross-sectional functional differences between the peripheral and central lung in this disease have not been well investigated using an imaging technique. In this study, perfusion single-photon emission tomography (SPET) and the recently developed dynamic xenon-133 SPET were applied to investigate the cross-sectional functional differences in pulmonary emphysema in smokers [14, 15, 16]. The results were also compared

Correspondence to: K. Suga, Department of Radiology, Yamaguchi University School of Medicine, 1-1-1 Minamikogushi, Ube, Yamaguchi 755-8505, Japan, Tel.: +81-836-222283, Fax: +81-836-222285

with morphological density-mask CT images, which specifically visualized the distribution of abnormally low attenuation lung areas (LAAs) indicative of emphysematous changes [17].

Materials and methods

Study populations. The subjects were 81 patients (76 males and 5 females; mean age 64.1±4.7 years; range 43–78), who underwent perfusion SPET and dynamic ^{133}Xe SPET between April 1993 and October 1999 in our hospital to evaluate regional lung function for relatively advanced pulmonary emphysema. All these patients had a history of long-term cigarette smoking, ranging from 460 to 1840 on the Brinkman index (cigarette consumption per day × years). The diagnosis of pulmonary emphysema was based on thin-slice, high-resolution CT scans, physical findings and pulmonary function tests (PFTs). On PFTs, the mean values of predicted vital capacity (%VC) and forced expiratory volume in 1 s (%FEV_1) were 71.4%±10.3% and 43.3%±11.9%, respectively.

For comparison, six healthy non-smokers without a history of lung disease and with normal PFTs (four males and two females; mean age 51.2±3.2 years, range 45–57) and 17 non-smoker patients with various non-obstructive lung diseases (ten males and seven females; mean age 52.4±3.2 years, range 48–73), including eight with pulmonary thromboembolism, four with primary pulmonary hypertension, five with diffuse interstitial lung disease (four with usual interstitial pneumonia, one with desquamative interstitial pneumonia), were also studied. Informed consent was obtained from all of the participants under an institutionally approved human subjects research protocol.

^{99m}Tc-MAA SPET. Perfusion SPET was performed using a triple-detector SPET system with a high-resolution, low-energy collimator approximately 10 min after the ^{133}Xe SPET study described below. After injection of 185 MBq (5 mCi) of ^{99m}Tc-macroaggregated albumin (MAA) and with the patients in the same position as in a ^{133}Xe SPET study, the projection data were serially obtained by 60 projections over 360°, in a 64×64 matrix and using an energy window of 140 keV±20%. SPET data were reconstructed into three orthogonal planes exactly matched to the ^{133}Xe SPET slices, using a Butterworth prefilter (order no. 8, cut-off frequency 0.13 cycles/cm) and a ramp backprojection filter, with the same slice thickness as in the ^{133}Xe SPET images. After acquisition of the SPET images, planar perfusion images of eight views including anterior/posterior, right and left lateral, and left and right anterior and posterior 45° oblique, were obtained using a dual-head detector scinticamera with a high-resolution, low-energy collimator. The preset counts were 650 kcounts per image.

As shown in Fig. 1, lung perfusion distribution was classified into five patterns at each of the upper, middle and lower lung zones on perfusion SPET images. These patterns were: periphery-dominant perfusion with a stripe sign, central-dominant perfusion with peripheral perfusion defects, indeterminate due to uneven perfusion defects between the peripheral and central lung, well-preserved perfusion throughout the lung (over 80% of the lung area was well perfused) and defective perfusion throughout the lung (over 80% of the lung area was not perfused). A stripe sign was defined as the presence of a distinct curvilinear line or band of perfused lung tissue between a perfusion defect and the adjacent pleural surface, and was especially used as an indicator of preserved perfusion in the peripheral lung. A single SPET slice at approximately the middle level of each lung zone served for the comparison with the matched dynamic ^{133}Xe SPET and CT scan slices.

Dynamic ^{133}Xe SPET. Dynamic ^{133}Xe SPET was carried out using a triple-head SPET system with a return mode of continuous repetitive rotating acquisition, as described previously [14, 15, 16]. Briefly, after 5- to 6-min inhalation of ^{133}Xe gas (concentration; 60–72 MBq/l), an equilibrium and 10–12 subsequent washout images were acquired with an acquisition time of 30 s, and with 64×64 pixels and an energy window of 80 keV±20%. To eliminate the settling time between projections and acquisition of multiple temporal samples of data, each detector was continuously and repeatedly rotated clockwise (for 15 s), and counterclockwise (for 15 s) across the same projection arc. With the use of three detectors, a gantry rotation of 120° around the chest provided projections over a full 360° arc. Averaged projection data at the same angle (per 6°) in both directional rotations were used to reconstruct a single SPET image; therefore, the change in ^{133}Xe activity in the lungs during the 30-s acquisition period was averaged. ^{133}Xe SPET data were reconstructed into equilibrium and washout images in transaxial planes using a Butterworth prefilter (order no. 8, cut-off frequency 0.13 cycles/cm) and a ramp backprojection filter, with a slice thickness of 1 pixel (3.2 mm), gapless.

Using equilibrium ^{133}Xe SPET images, curvilinear regions of interest (ROIs) were manually placed over the outer one-fourth peripheral lung area along pleural surfaces and the corresponding central lung area in each lung zone (Fig. 2). The ^{133}Xe clearance curve obtained from each ROI was corrected for background ra-

Fig. 1. Classification of lung perfusion distributions on ^{99m}Tc-MAA SPET (the graduation of greyish colours represents the degree of lung perfusion: black represents the most well perfused lung areas, and white represents areas of defective perfusion). *A*, Periphery-dominant perfusion with a stripe sign; *B*, central-dominant perfusion with peripheral perfusion defects; *C*, indeterminate due to uneven perfusion defects between the peripheral and central lung; *D*, well-preserved perfusion throughout the lung (over 80% of the lung area was well perfused); *E*, defective perfusion throughout the lung (over 80% of the lung area was not perfused)

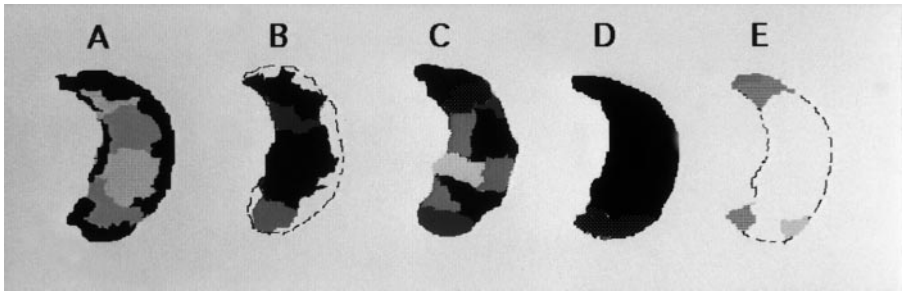

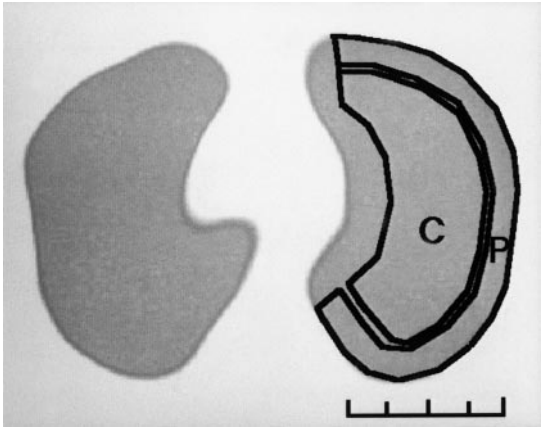

Fig. 2. ROIs used to quantify the ^{133}Xe clearance time on ^{133}Xe SPET. *P*, peripheral ROI; *C*, central ROI corresponding to the inner half of the lung

dioactivity as measured by a square ROI placed over the mediastinum, and the real half-time ($T_{1/2}$), defined as the ^{133}Xe clearance time required to reach the 50% level of the equilibrium count rate during washout, was calculated.

Chest CT scan. Chest high-resolution CT scanning was performed throughout the lung using a spiral scanner (Somatom Plus; Siemens, Erlangen, Germany), with contiguous 8-mm interval and 5-mm-thick sections. To objectively assess the extent and localization of low-attenuation areas (LAAs) representative of emphysematous changes, a density mask CT image of each lung section was automatically created by the supplemental software in the data processor. This density-mask CT image specifically visualized the LAAs with lung attenuation values of –960 Hounsfield units (HU) as a monotonous black colour. The lung and chest wall structures with lung attenuation values greater than –960 HU were presented in whitish colours. The cut-off level of –960 HU for the LAA was beyond 1 SD below the mean lung attenuation in our six healthy non-smokers, and was also consistent with the cut-off level used in a previous density-mask CT study [17].

The CT slice matched with the perfusion SPET slice was selected at the same cranio-caudal level after comparison of the scout view images of CT and perfusion SPET. Adequate correspondence was confirmed by comparing the landmarks of the mediastinal contours, such as the heart and aorta, and of the pulmonary hilar vessels, and the distance from the diaphragmatic contour. Although it might still have been difficult to exactly match CT and SPET slices, the effects of slight mismatching seemed inconsequential because each of the perfusion defects, or the emphysematous changes, similarly appeared in at least three or four adjacent sections above and/or below.

Image interpretation and data analysis. Two nuclear medicine (K.S. and N.K.), blind to the diagnosis and the information provided by the PFTs and the other imaging modalities in each subject, independently interpreted the patterns of perfusion distribution. Only a distinct stripe appearance was interpreted as positive for this sign, and if inconsistency was noted between the observers, it was judged to be negative. A chest radiology specialist (T.M.) interpreted the CT images, and the selection of CT slices that matched perfusion SPET slices was performed on the basis of con-

Table 1. Summary of the results of perfusion and ^{133}Xe SPET, and of density-mask CT in 486 lung zones in 81 smokers with pulmonary emphysema

Perfusion SPET	^{133}Xe clearance time (s)		Density-mask CT
	Central lung	Peripheral lung	
A Periphery-dominant perfusion with a stripe sign (*n*=288)	133.0±31.9	100.6±27.7*	Central-dominant LAA with LAA-spared peripheral lung (*n*=256) Uniform distribution of LAA throughout the lungs (*n*=29) Focal LAA only (*n*=3)
B Central-dominant perfusion with peripheral perfusion defects (*n*=117)	88.0±14.8	130.7±23.4*	Periphery-dominant LAA (*n*=104)
C Indeterminate (*n*=43)	120.4±32.1	121.0±19.3 (NS)	Uniform distribution of LAA throughout the lungs (*n*=36) Central-dominant LAA with LAA-spared peripheral lung (*n*=7)
D Well perfused throughout lung (*n*=25)	64.6±9.3	65.2±9.4 (NS)	Focal LAA only (*n*=25)
E Defective throughout lung (*n*=13)	247.8±57.8	244.1±39.6 (NS)	Uniform distribution of LAA throughout the lungs (*n*=10) Central-dominant LAA (*n*=3)

* $P<0.0001$ between the central and peripheral lung; NS, non-significant difference between the central and peripheral lung

sensus among the three observers. ^{133}Xe clearance times ($T_{1/2}$) were presented as mean values ± SD. The significance of the differences in the data comparisons between peripheral and central lung was assessed using the paired Student's *t* test, and the differences in the means between the groups was analysed using the unpaired Student's *t* test. A probability value of less than 0.05 was regarded as significant.

Results

Among a total of 486 lung zones in 81 smokers with pulmonary emphysema, a periphery-dominant perfusion pattern with a stripe sign was seen in 288 (59.2%) lung zones of 63 (77.7%) patients on SPET images (Table 1, Figs. 3, 4). Twenty-four of these stripe sign-positive zones were not detected on planar images, and conversely, the six positive zones on planar images were not identified on SPET images. This sign was more frequently seen in the lateral and/or dorsal portions of the middle and lower lung zones (*n*=211, 73.2%) than in the upper lung zone. In these lung zones with a stripe sign, the ^{133}Xe clearance time ($T_{1/2}$) was significantly prolonged in the central lung compared with the peripheral lung (P<0.0001) (Table 1). On the density-mask CT images, 256 (88.8%) of these lung zones showed central-dominant LAA distributions (Fig. 3), while the remaining zones showed uniform LAA distributions (*n*=29) or only focal LAAs in the central lung (*n*=3) (Fig. 4).

Conversely, 117 (24.0%) lung zones of 19 (23.4%) smokers with pulmonary emphysema showed a central-dominant perfusion pattern (Table 1), with significantly prolonged $T_{1/2}$ in peripheral lung (P<0.0001) and peripheral-dominant LAA distributions. The remaining 81 lung zones did not show any regional preference of perfusion defects (Table 1). In these lung zones, LAA distributions were central-dominant in seven with an indeterminate pattern, and in three with a defective perfusion pattern. However, LAA distributions did not show any regional preference in the remaining zones. Overall, there was no significant difference in $T_{1/2}$ between the peripheral and central lung, although $T_{1/2}$ was faster in the peripheral lung in seven lung zones with an indeterminate pattern, in five with a well-preserved perfusion pattern and in three with a defective perfusion pattern. Compared with the average $T_{1/2}$ in the periphery lung of 288 lung zones with a stripe sign, that in 13 lung zones with a defective perfusion pattern was significantly prolonged (P<0.0001), while the value in 25 well-preserved lung zones was, conversely, faster (P<0.0001) (Table 1).

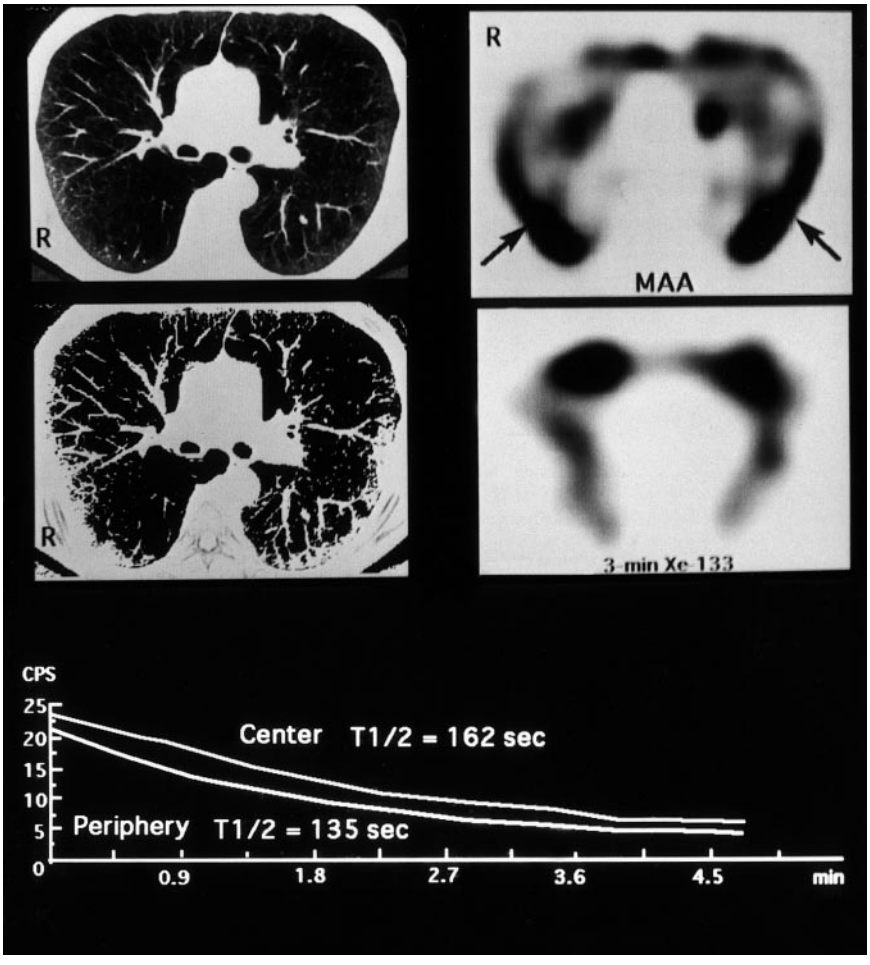

Fig. 3. A 63-year-old man with a smoking index of 1305. Chest CT scan (*top left*) shows diffuse emphysematous changes throughout the lungs. The density mask CT image (*middle left*) shows central-dominant LAA distributions (*black*) with linear or band-like LAA-spared lung tissues in the peripheral lung. ^{99m}Tc-MAA SPET (*top right*) shows periphery-dominant perfusion with a stripe sign (*arrows*), while central lung perfusion is markedly reduced. ^{133}Xe SPET image 3 min after initiation of washout (*middle right*) shows ^{133}Xe retention predominantly in the central lung area. The time-activity curves in the left lung (*bottom*) show faster ^{133}Xe clearance time ($T_{1/2}$) in the peripheral lung area than in the central lung area

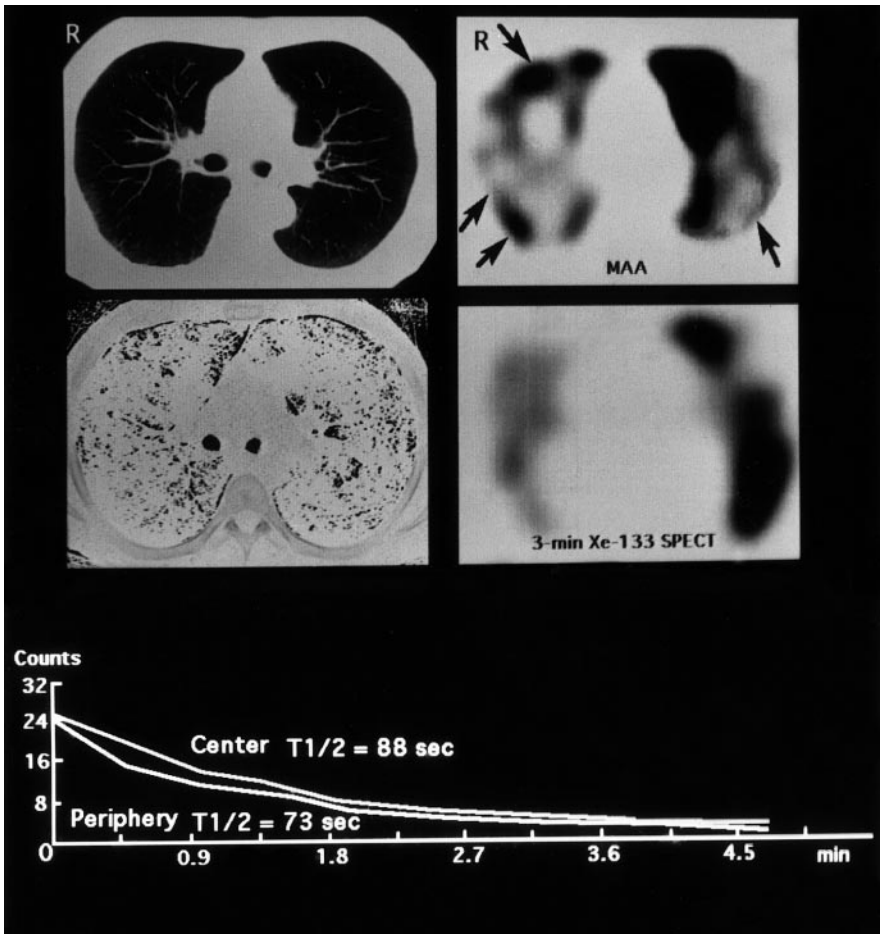

Fig. 4. A 56-year-old man with a smoking index of 580. Chest CT scan (*top left*) does not show noticeable abnormalities in the lungs. The density mask CT image (*middle left*) shows only focal LAA, which is nearly even between peripheral and central lung. ^{99m}Tc-MAA SPET (*top right*) shows periphery-dominant perfusion with a stripe sign (*arrows*). ^{133}Xe SPET image 3 min after initiation of washout (*middle right*) shows heterogeneous ^{133}Xe retention throughout the lung. The time-activity curves in the right lung (*bottom*) show faster $T_{1/2}$ in the peripheral lung area than in the central lung area

In six healthy non-smokers, the stripe sign was absent and the average $T_{1/2}$ was 39.9±7.3 s, without any significant difference between the central and peripheral lung (41.2±8.2 s vs 38.7±6.3 s; NS). In 102 lung zones of 17 patients with non-obstructive lung diseases, the stripe sign was also absent, and there was no significant difference in $T_{1/2}$ between the central and peripheral lung (75.3±38.2 s vs 81.5±26.4 s; NS). LAAs were absent or only focal without regional preference in these patients.

Discussion

This study showed a high incidence of a stripe sign on perfusion SPET in the smokers with pulmonary emphysema, with significantly faster ^{133}Xe clearance and preserved CT attenuation in the peripheral lung. By contrast, regional preferences with respect to perfusion and ventilation abnormalities and LAA distributions were absent in patients with non-obstructive lung diseases. These results may indicate low susceptibility of pathological development of smoking-related pulmonary emphysema in the peripheral lung parenchyma.

Pulmonary emphysema often occurs non-uniformly in the lungs, and this disease can be classified into central and peripheral types on cross-sectional CT images [3, 4, 5, 6]. The predilection of emphysematous changes for central lung in our patients may be related to their long-term smoking histories [7, 8, 9, 11]. The difference in the susceptibility to emphysematous changes between peripheral and central lung can be explained by structural differences in pulmonary lobules and by non-uniform lung damage caused by smoking. Compared with central pulmonary lobules, peripheral lobules are relatively large, relatively uniform in shape and marginated by thicker and better-defined interlobular septa [1]. Because of instability of interlobular septa in the central lung, emphysematous changes might spread more easily in this area. A predisposition towards overinflation of the central lung might compress peripheral lung tissues, resulting in higher attenuation on CT images. Turnover of neutrophils and macrophages, which phagocytize inhaled toxic smoke particles, would liberate excessive amounts of elastase or oxidants predominantly in the central lung, leading to more marked emphysematous destruction [5, 6]. By contrast, the relatively longer interaction with slower blood flow including antiprotease in the peripheral lung as compared with the central lung may protect against emphysematous destruction in the peripheral lung [5, 6].

A stripe sign seems characteristic for pulmonary emphysema, and this sign has only occasionally been seen in lung disorders other than this disease [7, 8, 13]. In pulmonary emphysema, lung perfusion in more severely unventilated and hyperinflated central lung should be reduced by hypoxic vasoconstriction and by increased vascular resistance due to the mechanical effects of reduced volume on the extra-alveolar vessels. Central emphysematous destruction may not interrupt blood flow supply to the relatively well ventilated peripheral lung because of the persistence of numerous surviving side branches to distal arterioles [18]. This is compatible with the clinical observations of normal pulmonary artery pressure and a low incidence of right ventricular hypertrophy in patients with advanced pulmonary emphysema [19, 20]. The regional preference of the stripe sign for the middle and lower lung zones may be partly related to the gravitational effects on lung perfusion; the preserved perfusion of emphysema-spared peripheral lung compared with the central lung can be more stressed by a higher proportion of pulmonary perfusion in these lung zones. In addition to decreased perfusion, lung destruction should be more severe in the upper lung zone because of a higher gravitational mechanical stress.

The false-negative or false-positive stripe sign cases on planar perfusion images support the superiority of SPET imaging in the detection of this sign [10, 13]. In contrast to the results of this ^{133}Xe SPET study, previous planar studies have shown the presence of ventilation abnormalities in only 50%–72% of the lung zones with a stripe sign [3, 7, 8]. This difference in detection rates may be due to the different sensitivities of the imaging techniques. The two-dimensional character of planar imaging inherently limits its sensitivity and accuracy [1, 3, 14, 15]. As indicated by some disparities between the lung function and morphology in our patients, cross-sectional perfusion and ^{133}Xe SPET studies seem indispensable for the accurate assessment of lung impairment in pulmonary emphysema. Lung function can be heterogeneously impaired despite a uniform or normal CT appearance [14, 15]. This is because localized alveolar destruction of less than 5 mm in diameter cannot be identified on CT images owing to the limited spatial resolution [16, 21, 22, 23, 24, 25, 26].

The major pathology in our patients was probably related to the centrilobular type emphysema usually associated with smoking [2]. Specific classification of pathological subtypes, however, is difficult on CT images in advanced pulmonary emphysema because of the confluent appearance of emphysematous tissues and loss of regional preference [2, 4, 6]. To clarify which subtypes of emphysema predominantly show the central type of emphysema over time, cross-sectional development of this disease should be investigated. The use of a combination of perfusion and ^{133}Xe SPET will be helpful for this purpose.

Acknowledgements. This study was supported in part by a Grant for Scientific Research (08671033) from the Japanese Ministry of Education.

References

1. Webb WR, Muller NL, Naidich DP, eds. *High-resolution CT of the lung. 2nd edn.* Pennsylvania: Lippincott-Raven; 1996: 23–40.
2. Webb WR, Muller NL, Naidich DP, eds. *High-resolution CT of the lung. 2nd edn.* Pennsylvania: Lippincott-Raven; 1996: 234–240.
3. Goddard PR, Nicholson EM, Laszlo G, Watt I. Computed tomography in pulmonary emphysema. *Clin Radiol* 1982; 33: 379–387.
4. Naidich DP, Zerhouri EA, Siegelman SS. *Computed tomography of the thorax.* New York: Raven; 1984: 226–238.
5. Thurlbeck WM. Chronic airflow obstruction. In: Thurlbeck WM, ed. *Pathology of the lung.* Stuttgart New York: Thieme Medical; 1988: 519–575.
6. Martelli NA, Hutchison DCS, Barter CE. Radiological distribution of pulmonary emphysema. Clinical and physiological features of patients with emphysema of upper or lower zones of lungs. *Thorax* 1974; 29: 81–89.
7. Sostman HD, Gottschalk A. The stripe sign: a new sign for diagnosis of nonembolic defects on pulmonary perfusion scintigraphy. *Radiology* 1982; 142: 737–741.
8. Sostman HD, Gottschalk A. Prospective validation of the stripe sign in ventilation-perfusion scintigraphy. *Radiology* 1992; 184: 455–459.
9. Murata K, Itoh H, Senda M, Noma S, Togo G, Yonekura Y, Nishimura K, Izumi T, Oshima S, Torizuka K. Stripe sign in pulmonary perfusion scintigraphy: central pattern of pulmonary emphysema. *Radiology* 1986; 160: 337–340.
10. Pace WM, Goris ML. Pulmonary SPECT imaging and the stripe sign. *J Nucl Med* 198; 39: 721–726.
11. Teates CD, Brookeman JR, Daniel TM, Truwit JD, Parekh JS, Mugler JP, De Lange EE. The stripe sign correlation of radionuclide ventilation and perfusion with He-3 magnetic resonance lung imaging. *Clin Nucl Med* 1999; 24: 747–750.
12. Magee M, Magnussen P, Chicco P. Mechanism for the stripe sign in a pulmonary scintigraphy model. *J Nucl Med* 1997; 38: 299P.
13. Feldman DR, Schabel SI. Pseudostripe sign in lobar collapse. *J Nucl Med* 1996; 37: 1682–1683.
14. Suga K, Nishigauchi K, Kume N, Kioke S, Takano K, Matsunaga N. Regional ventilatory evaluation using dynamic imaging of xenon-133 washout in obstructive lung disease: an initial study. *Eur J Nucl Med* 1995; 22: 220–226.
15. Suga K, Nishigauchi K, Kume N, Koike S, Takano K, Tokuda O, Matsumoto T, Matsunaga N. Dynamic pulmonary SPECT of xenon-133 gas washout. *J Nucl Med* 1996; 37: 807–814.
16. Suga K, Nishigauchi K, Kume N, Takano K, Koike S, Shimizu K, Matsunaga N. Pulmonary dynamic densitometry acquired by spiral CT to detect ventilation abnormalities in obstructive airway disorders: comparison with dynamic Xe-133 SPECT. *Radiology* 1997; 202: 855–862.
17. Sakai N, Mishima M, Nishimura K, Itoh H, Kuno K. An automated method to assess the distribution of low attenuation areas on chest CT scans in chronic pulmonary emphysema patients. *Chest* 1994; 106: 1319–1325.

18. Reid JA, Heard B. The capillary network of normal and emphysematous human lungs studied by injections of Indian ink. *Thorax* 1963; 18: 201–212.
19. Mounsey JP, Ritzmann LW, Selversione NJ, Briscoe WA, MeLernore GA. Circulatory changes in severe pulmonary emphysema. *Br Heart J* 1952; 14: 153–157.
20. Vizza CD, Lynch JP, Ochoa LL, Richardson G, Trulock EP. Right and left ventricular dysfunction in patients with severe pulmonary disease. *Chest* 1998; 113: 576–583.
21. Alderson PO, Lee H, Secker-Walker RH, Forrest JV. Detection of obstructive pulmonary disease. Relative sensitivity of ventilation-perfusion studies and chest radiography. *Radiology* 1974; 111: 643–648.
22. Alderson PO, Biello DR, Sachariah KG, Siegel BA. Scintigraphic detection of pulmonary embolism in patients with obstructive pulmonary disease. *Radiology* 1981; 138: 661–666.
23. Morrell NW, Roberts CM, Biggs T, Seed WA. Collateral ventilation and gas exchange in emphysema. *Am J Respir Crit Care Med* 1994; 150: 635–641.
24. Miller RP, Muller NL, Vedal S. Limitations of computed tomography in the assessment of emphysema. *Am Rev Respir Dis* 1989; 139: 980–983.
25. Kuwano K, Matsuba K, Ikeda T, Murakami J, Araki A, Shigematsu Nl. The diagnosis of mild emphysema: correlation of computed tomography and pathology scores. *Am Rev Respir Dis* 1990; 141: 169–178.
26. Chicco P, Magnussen JS, Palmer AW, Mackey DW, Van der Wall H. Threshold of detection of diffuse lung disease. *J Nucl Med* 1999; 40: 85–90.